Zoological Journal of the Linnean Society, 2018, **184**, 95–114. With 9 figures.

Redescription and phylogenetic reassessment of *Asialepidotus shingyiensis* (Holostei: Halecomorphi) from the Middle Triassic (Ladinian) of China

GUANG-HUI XU[1,*] and XIN-YING MA[1,2]

[1]*Key Laboratory of Vertebrate Evolution and Human Origins of Chinese Academy of Sciences, Institute of Vertebrate Paleontology and Paleoanthropology, Chinese Academy of Sciences, Beijing 100044, China*
[2]*University of Chinese Academy of Sciences, Beijing 100049, China*

Received 17 September 2017; revised 5 November 2017; accepted for publication 17 November 2017

The previously alleged ‘semionotid’ fish *Asialepidotus shingyiensis* from the Middle Triassic (Ladinian) marine deposits of Guizhou and Yunnan, China has recently been identified as a halecomorph, but its phylogenetic relationships with other halecomorphs remain controversial. This taxon was successively placed in different halecomorph orders: Amiiformes, Parasemionotiformes and ‘Panxianichthyiformes’. Here, a detailed redescription of *Asialepidotus* is presented based upon a comparative study of the original material with 50 new specimens. Newly recognized anatomical information includes a V-shaped rostral, paired vomers, a toothed parasphenoid, a dermosphenotic with a canal-bearing innerorbital flange, a splint-like quadratojugal, a branch of the infraorbital sensory canal in the maxilla, and many elements in the hyoid and branchial apparatuses and the lower jaw. Results of a cladistic analysis incorporating these new data indicate that the ‘Panxianichthyiformes’ is a poorly defined, paraphylectic grade; *Asialepidotus* is not sister to *Panxianichthys* as previously suggested; instead, it is more derived than *Panxianichthys* and consists of the sister taxon of the clade *Robustichthys* plus Jurassic–Cretaceous ionoscopiforms. This phylogenetic reassessment of *Asialepidotus* extends the stratigraphic range of the Ionoscopiformes in China by ~4 Myr and supports the hypothesis that the early ionoscopiform diversification was already established by the Middle Triassic.

ADDITIONAL KEYWORDS: evolution – fossils – neopterygian – osteology – phylogeny.

INTRODUCTION

Halecomorphi, Ginglymodi and Teleostei comprise the crown-group Neopterygii, the largest group of living vertebrates (Nelson, Grande & Wilson, 2016). The close relationships between Ginglymodi and Halecomorphi were originally recognized in 1861 when the living Holostei were restricted to include only *Lepisosteus* and *Amia* (Huxley, 1861; followed by Regan, 1923; Goodrich, 1930; Romer, 1945; Nelson, 1969). Gardiner (1960) first proposed that *Amia* and teleosts might be descended from a common ancestor not shared with *Lepisosteus*. This hypothesis was later widely accepted (Rosen *et al*., 1981; Gardiner, 1984; Grande & Bemis, 1998; Liem *et al*., 2001; Nelson, 2006), since it was more clearly expressed by Patterson (1973), who grouped Halecomorphi and Teleostei into his coined Halecostomi. Another hypothesis that places Ginglymodi as the sister group of Teleostei has also been proposed (Olsen, 1984), but it is very weekly supported and has rarely been accepted. In the last decade, however, the Halecostomi concept has been challenged; recent analyses based on both morphological and molecular data consistently support sister-group relationships between Halecomorphi and Ginglymodi and, consequently, the Holostei concept was resurrected (Inoue *et al*., 2003; Hurley *et al*., 2007; Grande, 2010; Nakatani *et al*., 2011; Xu & Wu, 2012; Near *et al*., 2012; Broughton *et al*., 2013; Cavin, Deesri & Suteethorn, 2013; Deesri *et al*., 2014; Xu, Zhao & Coates, 2014; Xu & Shen, 2015; Nelson *et al*., 2016; Sun *et al*., 2017; Ma & Xu, 2017).

However, the origin and early evolution of Holostei remains obscure. This is largely because the accurate identification of a holostean taxon is difficult in their

---

*Corresponding author. E-mail: xuguanghui@ivpp.ac.cn early fossil record. The placement of the early Permian (Artinskian) *Brachydegma* in the Halecomorphi (Hurley *et al*., 2007) was rejected in subsequent studies (Near *et al*., 2012; Xu *et al*., 2014; Argyriou, 2017). The late Permian (Wuchiapingian) 'semionotid'-like taxon *Acentrophorus* promisingly represents the oldest holostean, but desperately needs restudy and formal analysis (Gill, 1923; Gardiner, 1960; Friedman, 2015). Holostei that underwent a rapid radiation in the aftermath of the end-Permian mass extinction (Benton *et al*., 2013; Friedman, 2015) have a rich fossil record in Triassic deposits, but many of them are taxonomically controversial and need detailed description and revision.

Asialepidotus shingyiensis Su, 1959 from the Middle Triassic (Ladinian) of China is such a taxonomically controversial holostean that badly needs revision. This taxon, originally regarded as the oldest semionotid in China (Su, 1959; Chang & Jin, 1996), was named on the basis of a single incomplete specimen from the lower part of the Zhuganpo Member of the Falang Formation exposed in the Dingxiao, Xingyi, Guizhou Province. Based on three nearly complete specimens from the same fossiliferous level, Liu *et al*. (2003) named *Guizhouella analilepida* and placed it into the halecomorph family Eugnathidae (= Caturidae, Amiiformes); this genus was later renamed as *Guizhoueugnathus* by Liu (2004) because the original name was preoccupied by a brachiopod genus. Jin (2009) first noticed that *G. analilepida* is probably a junior synonym of *A. shingyiensis* (subsequently supported by many others, e.g. Benton *et al*., 2013; Tintori *et al*., 2014; Sun *et al*., 2017; Xu & Ma, 2017) and he suggested the placement of *Asialepidotus* in the Parasemionotiformes. Additionally, Sun *et al*. (2017) regarded *Asialepidotus* as the sister taxon of *Panxianichthys* (Xu & Shen, 2015) and referred it to their named halecomorph order 'Panxianichthyiformes'. However, this hypothesis is not supported by others (Ma & Xu, 2017; Xu & Ma, 2017; see Discussion, below). Until recently, *Asialepidotus* has not been redescribed. Our comparative studies of the holotype, the three specimens previously studied by Liu *et al*. (2003), and 50 well-preserved specimens curated at the fossil collections of the Institute of Vertebrate Paleontology and Paleoanthropology (IVPP), Chinese Academy of Sciences, indicate that many morphological characteristics previously described for *Asialepidotus* were misidentified, and some significant features were unnoticed or undescribed (Su, 1959; Liu *et al*., 2003). A detailed redescription and revision of this taxon is presented in this paper.

GEOLOGICAL CONTEXT

Asialepidotus shingyiensis was recovered from the dark grey thin- to medium-bedded marlites and argillaceous limestones at the lower part of the Zhuganpo member of the Falang Formation exposed in the Dingxiao, Wusha and Baiwanyao of Xingyi, western Guizhou, and Shibalianshan of Fuyuan, and Changdi, Zhongshan and Banqiao of Luoping, eastern Yunnan, Southwest China (Su, 1959; Liu *et al*., 2003; Jin, 2006, 2009; Benton *et al*., 2013). Besides invertebrates and plants, the coexisting vertebrates include several other types of ray-finned fishes (Su, 1959; Jin, 2001, 2009; Liu, Yin & Wang, 2002; Liu *et al*., 2003; Xu *et al*., 2012; Tintori *et al*., 2014, 2015; Xu, Zhao & Shen, 2015), a coelacanth (Geng, Zhu & Jin, 2009) and diverse marine reptiles (Young, 1958; Li & Jin, 2003, 2009; Li, 2006; Benton, 2013; Li C *et al*., 2016). The whole fossil assemblage was named the Xingyi Fauna or Biota (Li, 2006; Benton *et al*., 2013).

Biostratigraphical studies of marine reptiles and ammonites suggest a late Middle Triassic (late Ladinian) age for the lower part of the Zhuganpo Member of the Falang Formation (Young, 1958; Chen, 1985; Li & Jin, 2003, 2009; Zou *et al*., 2015; Li C *et al*., 2016). This age determination has recently been supported by a zircon U-Pb age dating (240.8 ± 1.8 Mya) for the fossil beds (Li *et al*., 2016). Although a younger Late Triassic (Carnian) age was proposed by Wang *et al*. (1998) on the basis of conodont biostratigraphy, this was rejected by Zou *et al*. (2015), who commented that the conodont identification by Wang *et al*. (1998) is inaccurate.

MATERIAL AND METHODS

Most specimens in this study were mechanically prepared with sharp steel needles. In addition, several specimens (e.g. IVPP V22995 and V22996) were first mechanically prepared with needles and further prepared with dilute acetic acid. The X-ray scanning of IVPP V19998 was carried out using a micro-computed laminography system at the Key Laboratory of Vertebrate Evolution and Human Origins of Chinese Academy of Sciences. For better contrast, some specimens were dusted with ammonium chloride (NH_4Cl) or immersed in water when photographed. Illustrations were drawn manually and then prepared using Adobe Photoshop and Illustrator software packages (CS5). Tree searches were accomplished with the heuristic search algorithm in PAUP* 4.0b10 (Swofford, 2003). The relative position of fins and scale counts were expressed following Westoll (1944). Although we accept that actinopterygian frontals and parietals are the homologues of sarcopterygian parietals and postparietals, respectively (Schultze, 1993), we nevertheless use the traditional actinopterygian nomenclature, following Grande & Bemis (1998) and Grande (2010), for ease of comparison with most existing literature.

Besides 54 specimens of *A. shingyiensis* listed below, the following specimens were examined and compared for this study: *Calamopleurus cylindricus*, AMNH 11760, 11837, 11840 and FMNH PF9777, 11847, 14348, 14381, 14384, 14899; *Caturus furcatus*, FMNH UC2057; *Cyclurus kehreyi*, FMNH PF14073, 14377–14379; *Ikechaoamia meridionalis*, IVPP V5805.1; *Ionoscopus cyprinoides*, FMNH P15472; *Macrepistius arenatus*, AMNH 2435; *Ophiopsiella* (‘*Ophiopsis*’) *procera*, FMNH UC2037; *Oshunia brevis*, AMNH 12000, 12793; *Panxianichthys imparilis*, IVPP V19971, 19972 and GMPKU P3116–3119; *Robustichthys luopingensis*, IVPP V18568–18573 and ZMNH M1690, M1691; *Sinamia zdanskyi*, IVPP V1106, 1114.1; *Subortichthys triassicus*, IVPP V19003, 20051, 20052, 20680, 22950, 22951; and *Teffichthys* (‘*Perleidus*’) *madagascariensis*, NHMUK P16247, 16248, 19580–19584, 19587–19592, 19595–19599, 19603–19620, 19622, 19623.

ABBREVIATIONS

INSTITUTIONAL ABBREVIATIONS

AMNH, American Museum of Natural History, New York, NY, USA; FMNH, Field Museum of Natural History, Chicago, IL, USA; GMPKU, Geological Museum of Peking University, Beijing, China; IVPP, Institute of Vertebrate Paleontology and Paleoanthropology, Chinese Academy of Sciences, Beijing, China; NHMUK, Natural History Museum, London, UK; NIGP, Nanjing Institute of Geology and Palaeontology, Chinese Academy of Sciences; MES, Museum of Earth Sciences, Nanjing University; and ZMNH, Zhejiang Museum of Natural History, Hangzhou, China.

ANATOMICAL ABBREVIATIONS

ang, angular; ar, articular; ao, antorbital; ap, ascending process; apl, anterior pit-line; ar, articular; bf, basal fulcrum; bp, basipterygoid process; br, branchiostegal ray; cb, ceratobranchial; cha, anterior ceratohyal; chp, posterior ceratohyal; cl, cleithrum; clva, anterior clavicle element; clvb, posterior clavicle element; co, coronoid; cm, coronomeckelian; den, dentary; dp, dermopalatine; dpt, dermopterotic; dsp, dermosphenotic; ecp, ectopterygoid; enp, entopterygoid; es, extrascapular; ff, fringing fulcrum; fpa, fenestra for the palatine ramus of the facial nerve in premaxilla; fr, frontal; gu, gular; hb, hypobranchial; hh, hypohyal; hm, hyomandibula; hmf, foramen and groove for the hyomandibular trunk; hp, opercular process of hyomandibula; io, infraorbital; iop, interopercle; le, lateral ethmoid; mpl, middle pit-line; mpt, metapterygoid; mx, maxilla; mxc, sensory canal in maxilla; n, nasal; op, opercle; pa, parietal; par, prearticular; pas, parasphenoid; pcl, postcleithrum; pf, pectoral fin ray; pmp, posterior mandibular pit-line; pmx, premaxilla; pop, preopercle; ppl, posterior pit-line; pr, principal fin ray; pscl, presupracleithrum; pt, posttemporal; q, quadrate; qc, quadrate condyle; qj, quadratojugal; r, rostral; ra, retroarticular; rr, rudimentary fin ray; sa, supra-angular; sc, symplectic condyle; scl, supracleithrum; smx, supramaxilla; so, suborbital; sop, subopercle; sp, sphenotic; su, supraorbital; v, vomer.

MEASUREMENTS

BD, body depth; HL, head length; PAL, preanal length; PDL, predorsal length; PVL, prepelvic length; SL, standard length; TL, total length.

SYSTEMATIC PALAEONTOLOGY

ACTINOPTERYGII COPE, 1887

NEOPTERYGII REGAN, 1923

HOLOSTEI MÜLLER, 1845

HALECOMORPHI COPE, 1872

IONOSCOPIFORMES GRANDE & BEMIS, 1998

ASIALEPIDOTUS SHINGYIENSIS SU, 1959

Asialepidotus shingyiensis Su, 1959: 205, pl. III, figs. 1, 2. – Chang & Jin, 1996: 466. – Li & Jin, 2003: 796. – Chang & Miao, 2004: 538, fig. 3A (mislabeled as *Sinoeugnatus kueichowensis* in the figure legend). – Jin, 2009: 120, three figures (unnumbered). – Benton *et al*., 2013: 220, 221, fig. 20B. – Tintori *et al*., 2014: 400, fig. 8A. – Xu & Ma, 2017: 37, fig. 1.
Guizhouella analilepida – Liu *et al*., 2003: 350, pl. I, fig. 2; pl. IV, figs. 1, 2; pl. V, fig. 1; pl. VI, figs. 1, 2.
Guizhoueugnathus analilepida – Liu, 2004: 447.

Holotype: IVPP V2434, an incomplete, laterally compressed specimen, with most of the skull and caudal fin missing (Fig. 1).

Referred material: IVPP V 19005, 19009, 19996–19999, 20673–20679, 22856–22869, 22995–23000, 23002–23018; NIGP 136040 (Fig. 2), 136041; MES 3603.

Locality and horizon: Dingxiao and Wusha, Xingyi, Guizhou Province; Jiyang hills, Fuyuan, and Changdi, Luoping, Yunnan Province; Zhuganpo member of the Falang Formation, Ladinian, Middle Triassic.

Emended diagnosis: A large-sized ionoscopiform distinguished from other members of this order by the following combination of features: frontal nearly three times as long as parietal; parietal rectangular, slightly longer than wide; supraorbital sensory canal contacting anterior pit-line in parietal; dermopterotic 1.3–1.4 times as long as parietal; three (two, occasionally) pairs of extrascapulars; two supraorbitals; dermosphenotic with canal-bearing innerorbital flange; five infraorbitals; two suborbitals; quadratojugal splint-like; supramaxilla single, nearly

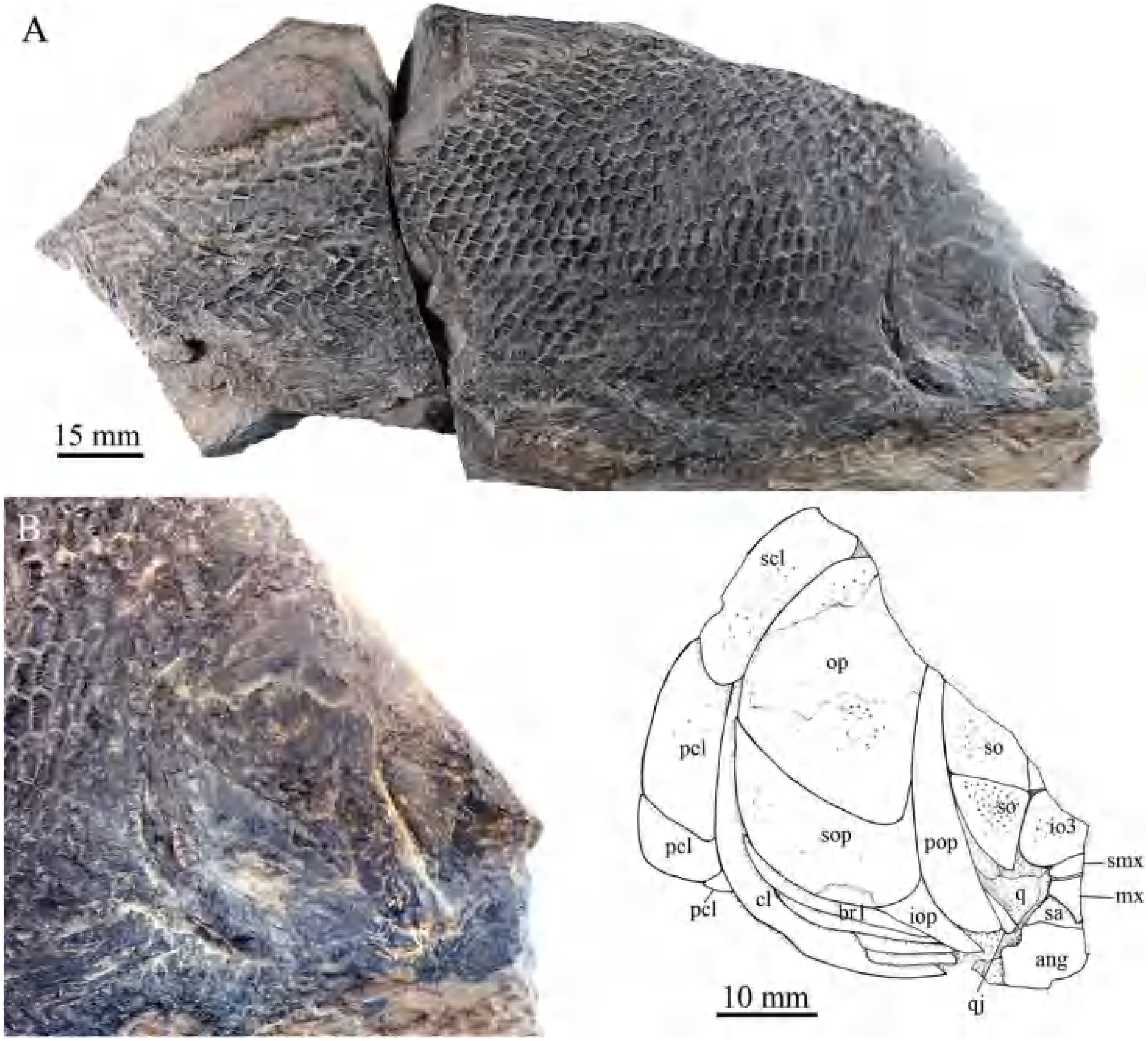

Figure 1. *Asialepidotus shingyiensis*, holotype (IVPP V2434). A, entire specimen. B, skull and pectoral girdle.

half of length of maxilla; maxilla with branch of infraorbital sensory canal; maxilla ending at level of posterior margin of orbit; 14 pairs of branchiostegal rays; median gular large and nearly triangular; 15 rays in each pectoral fin; 10–11 principal dorsal rays; 11–12 principal anal rays; 21–23 principal caudal rays; rhomboidal scales with serrated posterior margin; and scale formula of D25–26/P11–13, A22–24, C37–40/T43–45.

COMPARATIVE DESCRIPTION

General morphology and size

Asialepidotus has a blunt snout, a fusiform body and a moderately forked caudal fin (Figs 2–5). The dorsal fin inserts slightly posterior to the origins of pelvic fins. The anal fin is nearly equal to the dorsal fin in size. The great body depth lies midway between the posterior margin of the opercle and the origin of the dorsal fin. The smallest known specimen (IVPP V23003) is 60 mm in standard length (SL, the length from the tip of the snout to the posterior extremity of the caudal peduncle), and the largest specimen (IVPP V23010) reaches a SL of 273 mm. The head length (measured from the tip of the snout to the posterior margin of the opercle), accounting for 30–37% of SL, is relatively larger in small specimens than in large specimens (Table 1). The incompletely preserved holotype (Fig. 1) has a length of 125 mm from the posterior margin of the opercle to the posterior extremity of the caudal

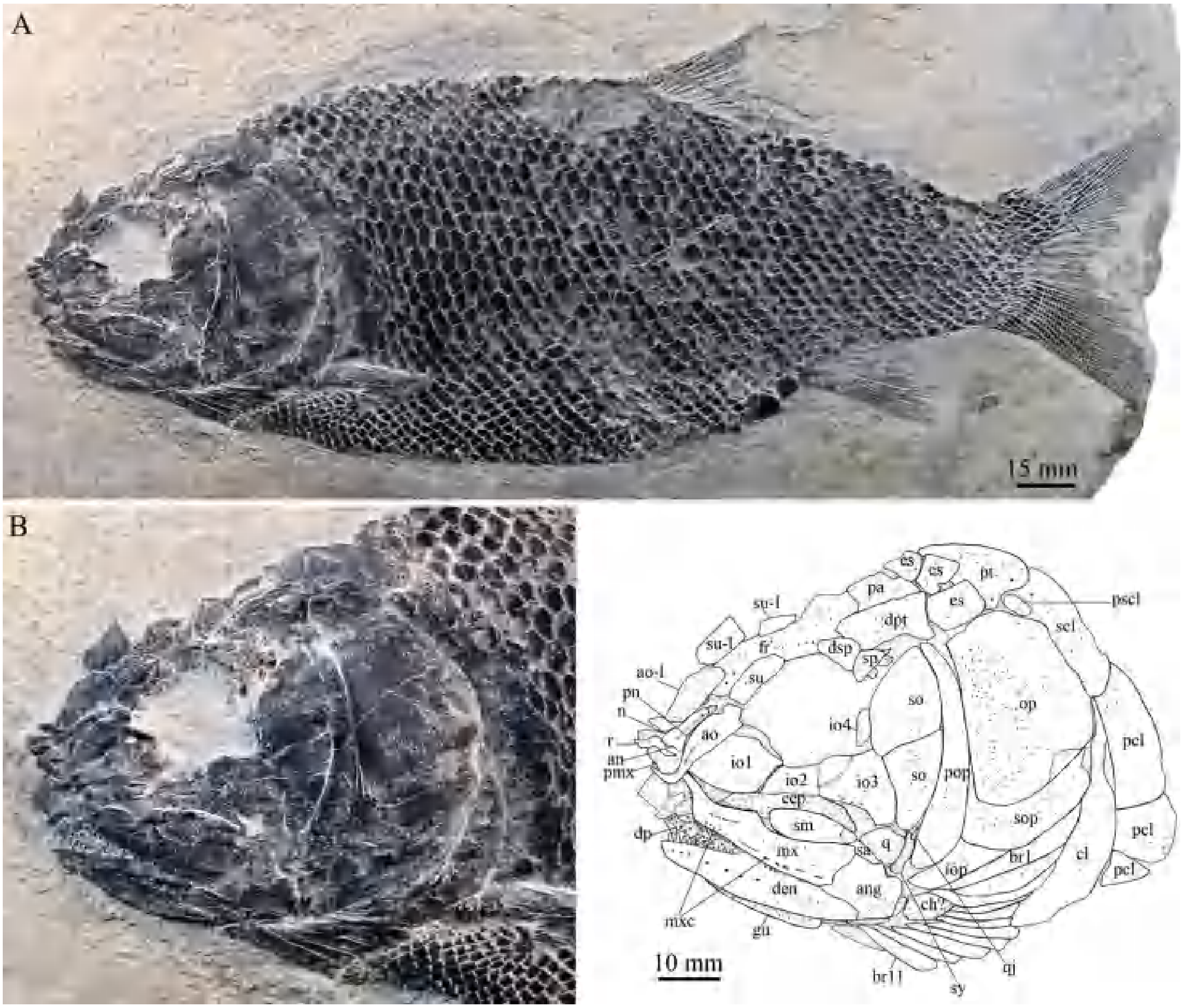

Figure 2. *Asialepidotus shingyiensis*, NIGP 136040. A, entire specimen. B, skull and pectoral girdle.

peduncle, and its SL is estimated to be ~190 mm. The outer surfaces of the cranial bones are ornamented with ganoine tubercles and ridges.

SNOUT

The canal-bearing bones of the snout consist of a median rostral and a pair of nasals and antorbitals (Figs 2–5). The rostral is narrow and nearly V-shaped, with a small posteriorly pointing median apex and a pair of lateral extensions. It overlies parts of the premaxillae anteriorly, and contacts the nasals posteriorly and the antorbitals laterally. The rostral houses the anterior commissure of the lateral line system, connecting the right and left sides to each other through the antorbitals. There is a sensory pore near the base of each lateral extension of this bone.

The paired nasals are elongate and taper posterodorsally. Each nasal contacts the rostral anteroventrally, the antorbital laterally and the frontal dorsally, and meets its counterpart along the middle line. The anterior margin of the nasal is slightly concave for the anterior nostril. The posterior nostril is located between the lateral margin of the nasal and the medial margin of the antorbital, resembling the condition in *Panxianichthys* (Xu & Shen, 2015). An anterior portion of the supraorbital sensory canal is enclosed in the nasal, indicated by several small pores on this bone.

The antorbitals are curved and elongate, having a tube-like anteroventral extension that contacts the rostral and an expanded posterodorsal portion that contacts the frontal and supraorbital. Posteriorly, it forms part of the anterior orbital margin, showing a condition as in *Subortichthys* (Ma & Xu, 2017),

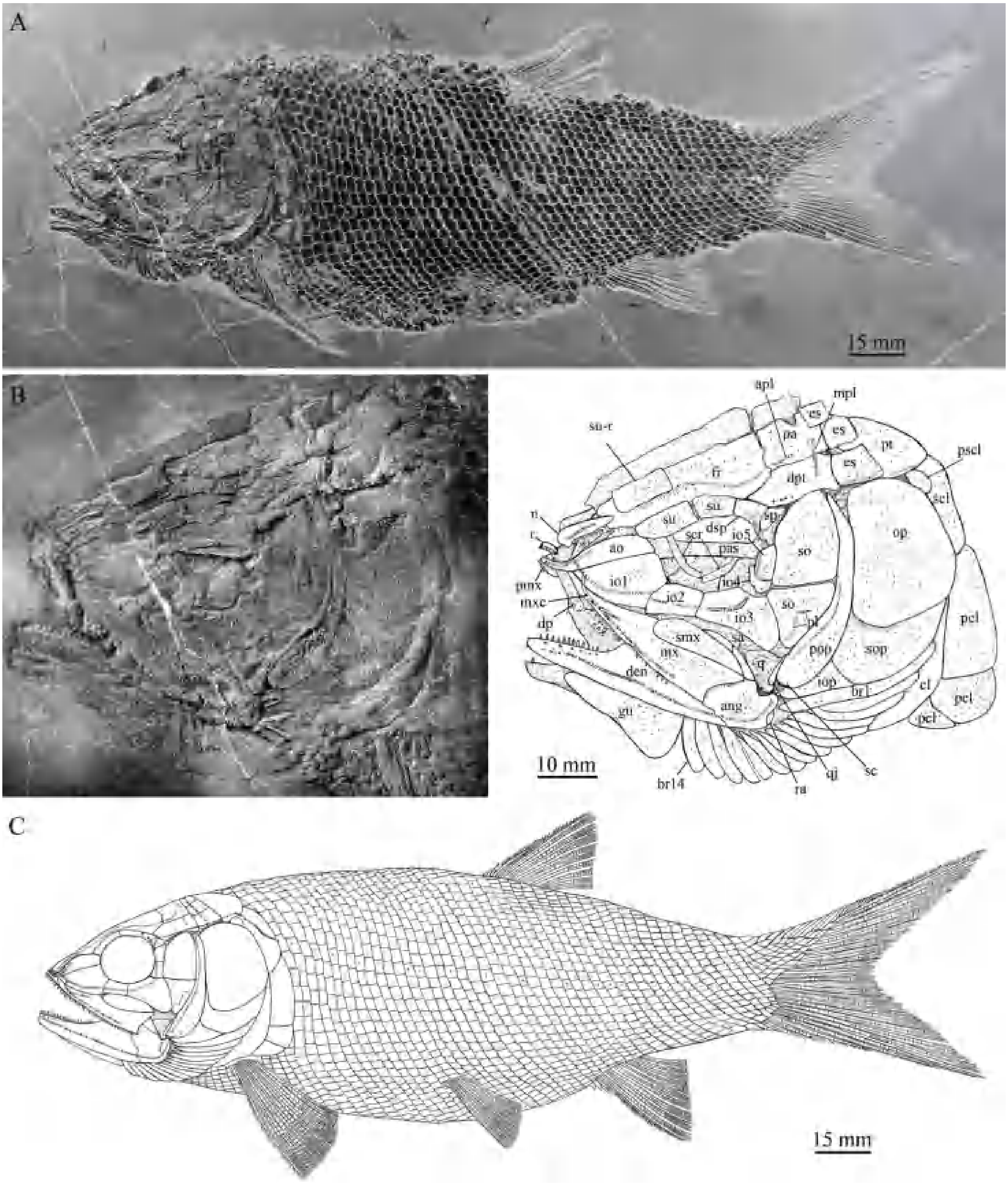

Figure 3. *Asialepidotus shingyiensis*. A, entire specimen, IVPP V23009. B, skull and pectoral girdle of A, dusted with ammonium chloride. C, reconstruction, based mainly on A.

Panxianichthys (Xu & Shen, 2015), *Robustichthys* (Xu *et al*., 2014), *Oshunia* (Maisey, 1991) and *Ophiopsis muensteri* (Lane & Ebert, 2012, 2015). In contrast, the antorbital is relatively short and does not reach the orbital margin in other ionoscopiforms. The conjunction of the ethmoid commissural canal and the infraorbital

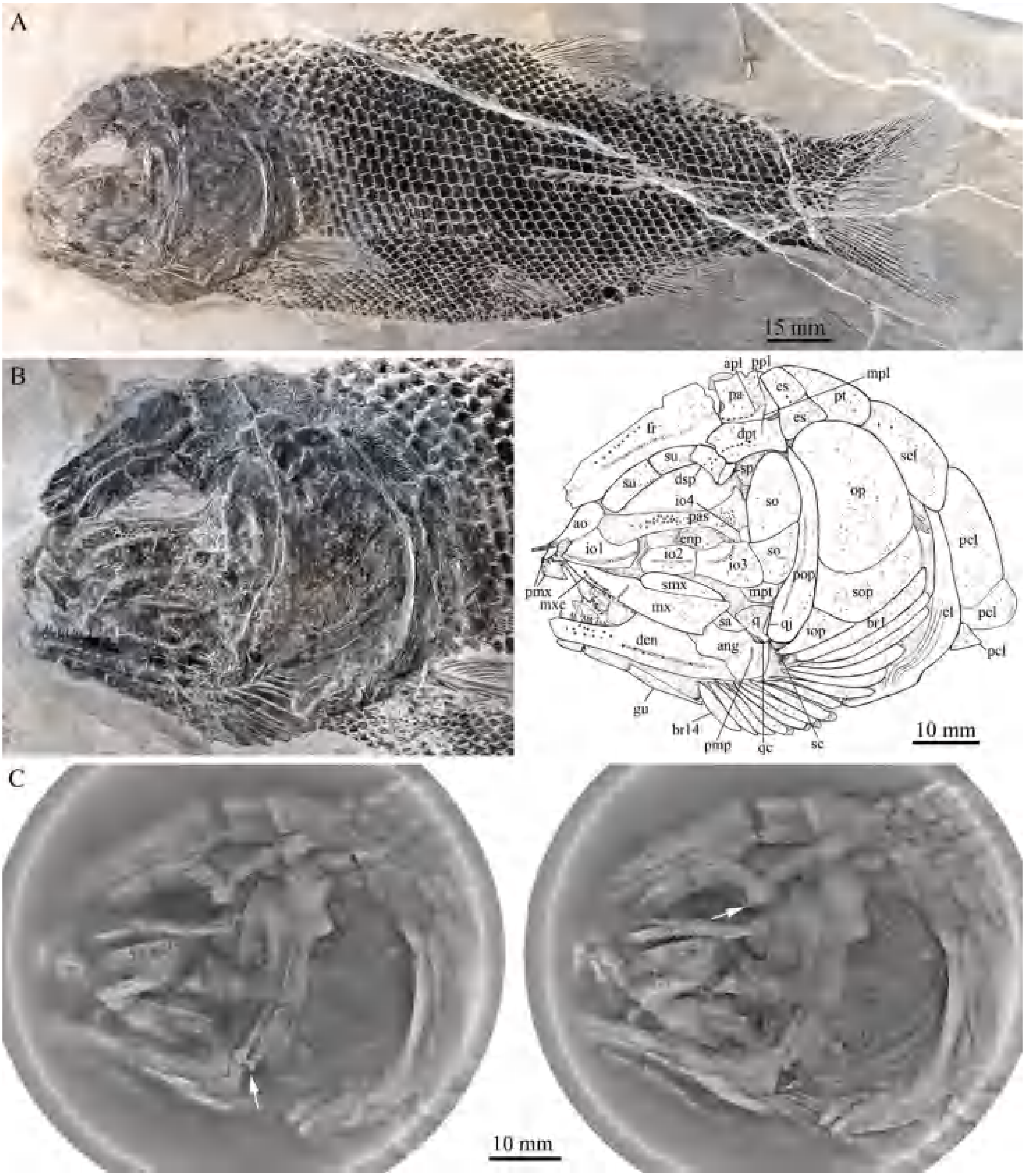

Figure 4. *Asialepidotus shingyiensis*, IVPP V19998. A, entire specimen. B, skull and pectoral girdle. C, two micro-computed scanning slices, with arrows showing the *Amia*-like double jaw articulation and the canal-bearing innerorbital flange of the dermosphenotic, respectively.

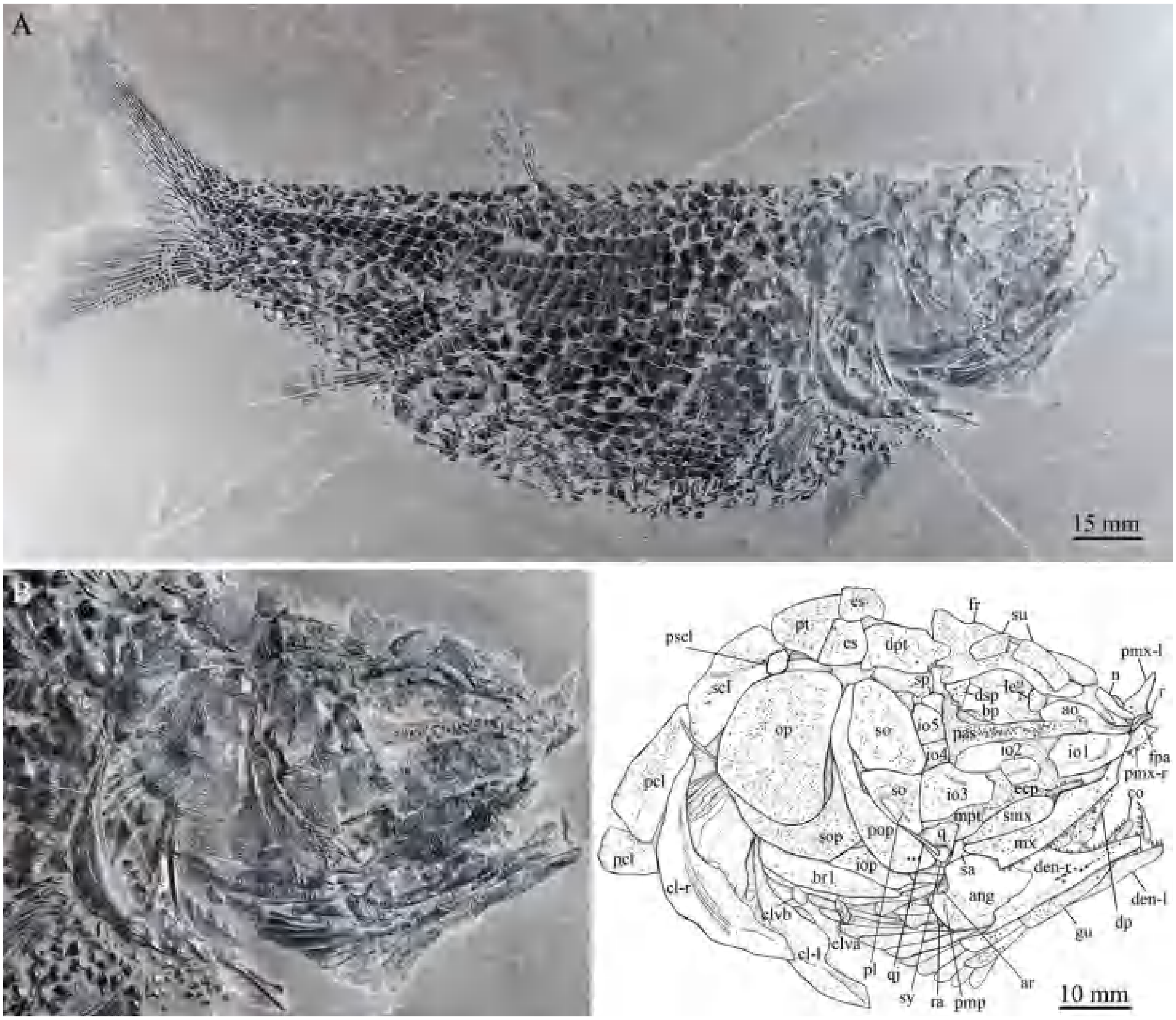

Figure 5. *Asialepidotus shingyiensis*, IVPP V22995. A, entire specimen. B, skull and pectoral girdle.

sensory canal is located at the anterior one-third portion of the antorbital.

SKULL ROOF

The skull roofing bones include a pair of frontals, parietals and dermopterotic, and three (two, occasionally) pairs of extrascapulars (Figs 2–5).

The elongate frontals are the largest elements on the skull roof. Each frontal is nearly three times as long as the parietal, having a slightly excavated lateral margin above the orbit, where it contacts the supraorbitals. The frontal widens posteriorly and contacts the parietal and the dermopterotic with a sinuous suture. The supraorbital sensory canal enters the frontal from the nasal, runs longitudinally through this bone, and enters the parietal posteriorly.

The paired parietals contact each other in a strongly digitated suture (Figs 3, 4). Each parietal is nearly rectangular, longer than wide. There is a straight, narrow zone where the extrascapulars lap onto the parietal. Three pit-lines are present. The anterior pit-line runs anteriorly near the lateral margin of this bone and contacts the supraorbital sensory canal in the frontal (Fig. 3). The middle pit-line extends from the posterolateral portion of the parietal, runs laterally into the dermopterotic, and ends near the temporal sensory canal in this bone. The posterior pit-line originates slightly anterior to the level of the middle pit-line, extends posterolaterally, and ends near the posterior margin of this bone.

The dermopterotic is elongate, with a tapered anterior process that fits a notch at the posterior portion

Table 1. Measurement data (in millimetres)

Specimen	SL	HL	BD	PVL	PDL	PAL	TL
V19998	173	52	63	104	110	135	210
V19999	116	41	47	73	77	95	152
V19005	189	59	69	114	117	146	235
V22995	191	63	69	116	121	152	247
V22996	122	42	50	71	76	95	167
V23002	64	24	22	39	41	53	88
V23003	60	22	20	36	37	47	77
V23004	88	30	33	53	57	68	117
V23005	105	35	40	63	67	81	136
V23006	149	48	58	91	95	122	192
V23007	143	47	54	86	89	116	181
V23008	175	55	67	107	113	140	233
V23009	190	63	71	111	119	148	248
V23010	273	91	112	163	173	217	335
V20675	169	55	65	99	101	133	219
V20676	247	77	100	140	157	184	309
V22862	150	43	64	86	94	115	189
V23016	184	57	74	111	118	148	231
V23017	160	47	63	90	97	123	206

BD, body depth; HL, head length; PAL, preanal length; PDL, predorsal length; PVL, prepelvic length; SL, standard length; TL, total length.

of the frontal (Fig. 5). The dermopterotic is 1.3–1.4 times as long as the parietal, to which it is sutured medially with a nearly straight margin. The lateral margin of the dermopterotic is excavated. The temporal sensory canal runs longitudinally through the dermopterotic near its lateral margin, and enters the lateral extrascapular posteriorly.

The extrascapulars are trapezoidal bones and vary in size and number. Most specimens have three pairs of extrascapulars (Figs 2, 3), as described by Liu *et al*. (2003). However, several specimens have only two pairs of extrascapulars (Figs 4, 5). This probably represents an intraspecific variation, because the other anatomical features are consistent in these specimens. The supratemporal commissure runs transversely through the extrascapulars, indicated by several small pores at the middle portions of these bones.

Circumorbital bones

There are two elongate supraorbitals. The anterior is 1.4–1.5 times as long as the posterior. Two supraorbitals are otherwise present in *Panxianichthys* and *Robustichthys* (Xu *et al*., 2014; Xu & Shen, 2015), but other ionoscopiforms generally have three or more supraorbitals (Bartram, 1975; Alvarado-Ortega & Espinosa-Arrubarrena, 2008; Machado *et al*., 2013; Lane & Ebert, 2015; Ma & Xu, 2017). Notably, *Oshunia* lacks any supraorbitals (Maisey, 1991), representing a particular case in this order.

Five infraorbitals are present (Figs 2–5). The anteriormost or first infraorbital (= lachrymal) is large and cleaver shaped. It tapers anteriorly, having a triangular anteroventral portion that inserts between the anterorbital and the maxilla. The dorsal margin that borders the anterorbital is nearly straight, and the ventral margin is slightly rounded and borders the anterior half of the maxilla. The posterior margin of the first infraorbital is slightly concave. The infraorbital sensory canal passes longitudinally through the bone near its ventral margin, and has a branch running into the maxilla.

The second infraorbital is small and nearly trapezoidal, with a convex anterior margin and a straight posterior margin. The ventral border of this bone is slightly concaved and contacts the anterior portion of the supramaxilla ventrally. The infraorbital sensory canal runs longitudinally through the ventral portion of the second infraorbital, about two-thirds of the way down from its dorsal margin.

The third infraorbital is large and nearly pentagonal. It contacts the posterior portion of the supramaxilla with a concaved ventral margin and the ventral suborbital with a convex posterior margin.

The fourth infraorbital is small and quadrangular. It is sutured to the third infraorbital with a convex ventral margin. This bone tapers dorsally and contacts the fifth infraorbital with a straight dorsal margin.

The last, fifth infraorbital is also small, equal to the fourth infraorbital in size (Figs 3, 5). It is nearly quadrangular, 1.6 times deeper than wide, with a convex ventral margin and a posteriorly inclined dorsal margin. The sensory canal runs dorsoventrally through the fourth and fifth infraorbitals near the anterior margins of both bones.

The dermosphenotic has a broad dorsal portion and a narrow ventral, innerorbital flange. The dorsal portion is trapezoidal, ornamented with tubercles and ridges. The ventral innerorbital flange is tube-like and smooth, through which the dermosphenotic receives the infraorbital sensory canal from the last infraorbital.

The sphenotic (= autosphenotic of Rayner, 1948), not fused with the dermosphenotic, has a small portion participating in the skull roof, as in many other holosteans (Olsen & McCune, 1991; Grande & Bemis, 1998; Grande, 2010; Cavin *et al*., 2013). This exposed portion is smooth on the surface. It is sutured to the dermosphenotic anterodorsally and makes up a posterodorsal portion of the orbital margin, resembling the condition in other ionoscopiforms (Bartram, 1975; Grande & Bemis, 1998; Alvarado-Ortega &

Espinosa-Arrubarrena, 2008; Xu *et al.*, 2014; see Gardiner, Maisey & Littlewood, 1996, for discussion on this feature).

There are two suborbitals. The upper is large and trapezoidal, with its anterior margin slightly overlapped by the fourth and fifth infraorbitals. The lower is slightly smaller and sub-triangular, tapered ventrally. It bears two pit-lines: the dorsal originates at the middle portion of the suborbital, extends posteriorly, and ends near the posterior margin of this bone; the venteral originates just below the anterior tip of the horizontal pit-line, extends ventrally parallel to the posterior margin of the middle suborbital, and ends at the ventral corner of this bone. Compared with other ionoscopiforms, *Asialepidotus* has the fewest number of suborbitals; *Subortichthys*, *Panxianichthys*, *Ophiopsis*, *Ionoscopus* and *Quetzalichthys* commonly have three suborbitals (Bartram, 1975; Alvarado-Ortega and Espinosa-Arrubarrena, 2008; Xu & Shen, 2015; Ma & Xu, 2017), *Macrepistius* has five suborbitals (Schaeffer, 1960), and *Teoichthys* and *Robustichthys* have eight or more suborbitals (Machado *et al*., 2013; Xu *et al*., 2014).

Two sclerotic bones are discernible near the orbital rim. They are proportionally narrower than those in *C. furcatus* (Grande & Bemis, 1998) but resemble those of *Panxianichthys* in size (Xu & Shen, 2015).

Given that the dermosphenotic is incorporated into the skull roof and posteroventrally sutured to the exposed portion of the sphenotic, Liu *et al*. (2003) misidentified the dermosphenotic as the ‘third supraorbital’ and the exposed portion of the sphenotic as a ‘dermosphenotic’. This kind of misidentification also occurred in Saint-Seine’s (1949) description of *Ionoscopus* and Schaeffer’s (1960, 1971) descriptions of *Macrepistius*, as already pointed out by Maisey (1991) and Gardiner *et al*. (1996), respectively. In addition, Liu *et al*. (2003) misidentified two suborbitals as part of the ‘infraorbitals’ in *Asialepidotus*.

VOMERS AND PARASPHENOID

The vomers are elongate, abutting the premaxillae anteriorly and the parasphenoid posteriorly. Teeth are present only on the anterior portion of each vomer (Fig. 6). They are conical, and slightly smaller than those on the premaxilla.

The parasphenoid is cross shaped, with a pair of small, laterally directed basipterygoid processes and well-developed ascending wings. A large patch of teeth with rounded tips covers most of the oral margin of this bone from the level of the ascending wings to that of articular surfaces for the vomers. There are no foramens for the internal carotid and/or afferent pseudobranchial arteries in this bone. The teeth on the anterior portion of the patch are notably larger than those on the posterior portion (Figs 4–6).

PALATINE, HYOID AND BRANCHIAL SERIES

The dermopalatines are small and elongate, bearing teeth similar to those on the vomers. The ectopterygoid, entopterygoid and metapterygoid are sutured to each other, and it is difficult to identify the boundaries between them in most specimens. Densely arranged teeth are present on their medial surfaces, most of which are styliform with rounded tips, except those near the lateral portion of the ectopterygoid, which are pointed. In size, the teeth on the entopterygoid and the anterior portion of the ectopterygoid are largest and those on the metapterygoid smallest (Fig. 6).

The quadrate is small and triangular, articulating with the lower jaw with a strong condyle (Figs 2–4). Most of the quadrate is exposed beneath the ventral margin of the third infraorbital and the lower suborbital, showing a condition similar to *Panxianichthys* (Xu & Shen, 2015) and *Subortichthys* (Ma & Xu, 2017) but different from *Robustichthys* (Xu *et al*., 2014) and other ionoscopiforms, in which most of the bone is covered laterally by the infraorbital, suborbital and/or maxilla.

The quadratojugal is splint-like, with a slightly expanded anteroventral portion and a tapered posterodorsal portion (Figs 3–5). It rests on the anterior edge of the ventral portion of preopercle, and medially, covers a short posteroventral portion of the quadrate (including part of the condyle) but does not take part in the jaw articulation, showing a condition similar to that in *Subortichthys* (Ma & Xu, 2017), *Panxianichthys* (G-H Xu, personal observation on GMPKU P3116) and some ginglymodians (López-Arbarello, 2012). A quadratojugal is absent in *Robustichthys* (Xu *et al*., 2014) and more derived ionoscopiforms.

The hyoid arches are best exposed in IVPP V22856 (Fig. 6), including paired hyomandibulas, symplectics, hypohyals, and anterior and posterior ceratohyals. The hyomandibula is hatchet shaped, having a relatively long, posteriorly directed opercular process that articulates with the opercle. The depth from the base of the opercular process to the dorsal margin of this bone is about one-third the depth of the whole hyomandibula. The hyomandibula bears a foramen at the level of the opercular process, through which the hyomandibular branch of the facial nerve might have passed.

The symplectic is rode-like (Fig. 6), resembling that in *Subortichthys* (Ma & Xu, 2017) and *Robustichthys* (Xu *et al*., 2014). It has an expanded dorsal portion, a slightly constricted middle portion, and a strong ventral condyle that is partly exposed beneath the ventral margin of the preopercle and articulates with the lower jaw.

The hypohyal is nearly square, contacting its opposite medially. A foramen for the afferent hyoidean artery is absent in this bone, as in other holosteans

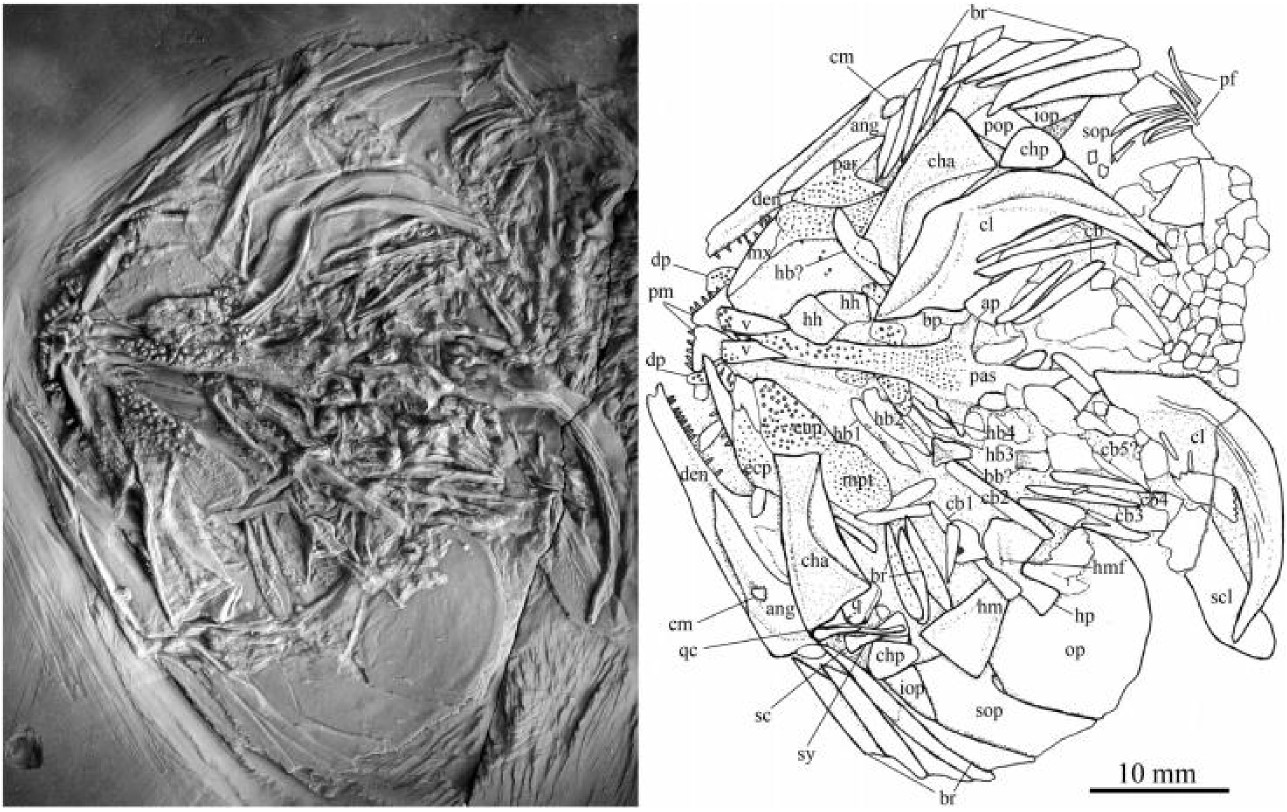

Figure 6. Skull and pectoral girdle of *Asialepidotus shingyiensis*, IVPP V22856, dusted with ammonium chloride.

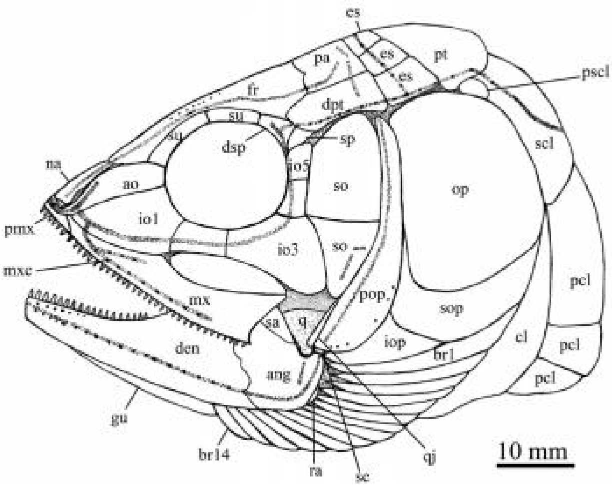

Figure 7. Reconstruction of skull and pectoral girdle of *Asialepidotus shingyiensis*.

and more primitive actinopterygians (Gardiner *et al.*, 1996; Grande & Bemis, 1998; Grande, 2010).

The anterior ceratohyal is elongate and large, ~60% the length of the lower jaw. It widens posteriorly and is proportionally broader than that in *Amia*. The posterior ceratohyal is small and subcircular.

Elements of the branchial arches are partly preserved in a few specimens, including four hypobranchials and five ceratobranchials on each side (Fig. 6). They are rod-like bones. Small tooth plates are discernible on the oral margins of some hypobranchials.

JAWS

The upper jaw is composed of a premaxilla, a maxilla and a supramaxilla (Figs 2–5, 7). The premaxilla is relatively large, having a horizontally expanded oral region and a deep, posterodorsally directed nasal process. A small foramen for the palatine ramus of the facial nerve lies slightly above the oral margin of the premaxilla (Fig. 5). There is no foramen for the olfactory nerve in the nasal process of this bone, showing a primitive condition as in *Watonulus* (Olsen, 1984) and *Robustichthys* (G-H Xu, personal observation). Eight teeth are present along the oral margin of the premaxilla. They are conical and nearly equal to those on the anterior portion of the maxilla in size.

The maxilla is elongate, having a notched posterior margin and a peg-like, medially directed anterior process, which extends between the premaxilla, the dermopalatine and the vomer (Fig. 6). The dorsal margin of the posterior part of the maxilla is concave,

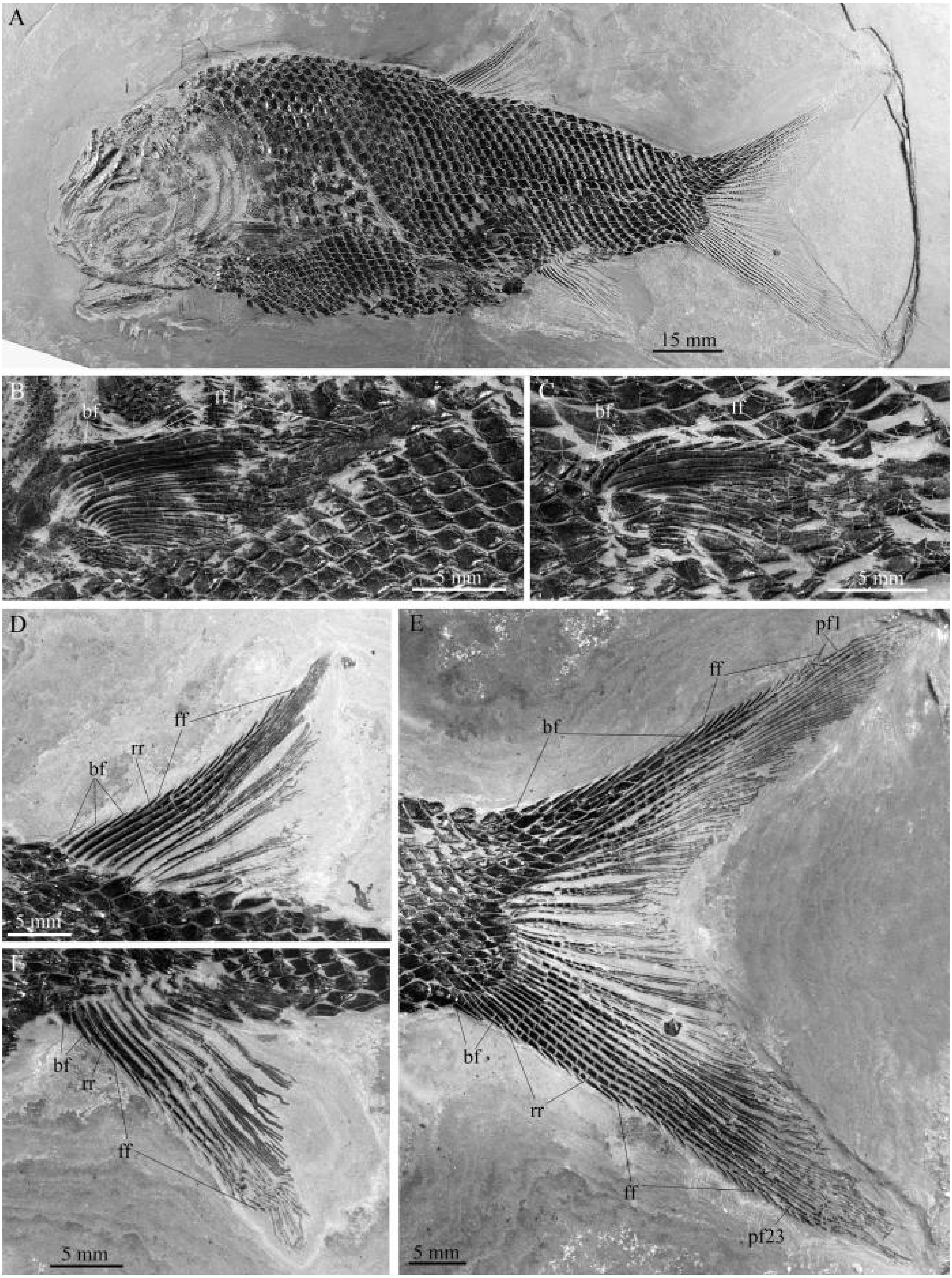

Figure 8. *Asialepidotus shingyiensis*, IVPP V22996. A, entire specimen. B, pectoral fin. C, pelvic fin. D, dorsal fin. E, caudal fin. F, anal fin. B–F, immersed in water when photographed.

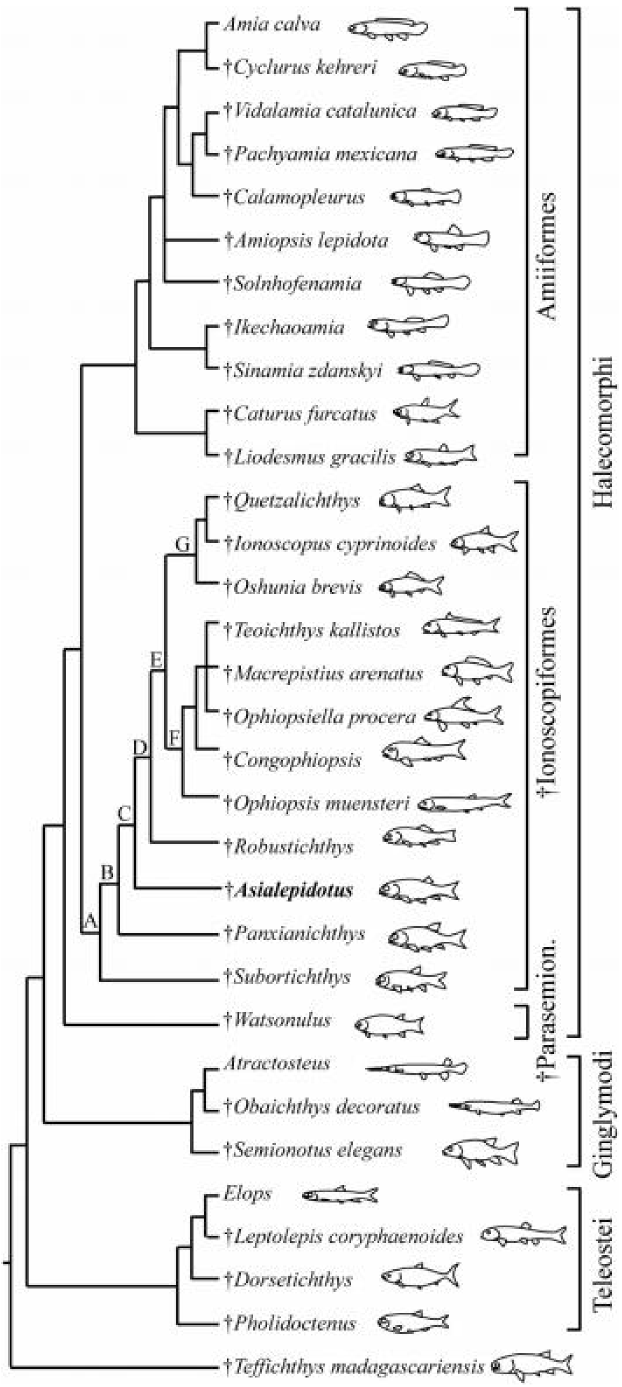

Figure. 9. Strict consensus of six most parsimonious trees, illustrating the phylogenetic position of *Asialepidotus* within the Neopterygii. Parasemion. = Parasemionotiformes. Character states supporting the clades include the following: A, 61(1)*, 78(1); B, 19(1); C, 64(1), 104(1); D, 82(1)*, 110(0); E, 4(1), 104(0); F, 1(1), 5(0), 51(1); and G, 75(1), 97(1). Character states marked with an asterisk have a consistency index of 1.0. For character descriptions, codings for the sampled taxa, and character states supporting all nodes and terminal taxa, see Parts S1–S3 of the Supporting Information.

into which the supramaxilla fits. The posterior end of the maxilla is located at the level of the posterior orbital margin. As in other ionoscopiforms, the maxilla encloses a branch of the infraorbital sensory canal that enters this bone from the first infraorbital. The branch passes through the anterior three-quarters of the length of the maxilla, indicated by a series of small pores and pits near the ventral margin of this bone (Fig. 3).

The supramaxilla is elongate and has rounded tips. It is about half the length of the maxilla.

The lower jaw is elongate and strong, bearing a large, dorsally expanded coronoid process at its posterior half portion. The maximal height of the lower jaw is 36–38% of its total length.

The dentary, the largest element of the lower jaw, is wedge shaped. It deepens posteriorly, forming the major part of the coronoid process.

The supra-angular is small and plate-like, forming a posterior portion of the coronoid process. In size, it is proportionally equal to the supra-angular of *Watsonulus* (Olsen, 1984) and smaller than that of *Amia* (Grande & Bemis, 1998).

The angular is trapezoidal and slightly over half of the length of the lower jaw, with its anterior portion laterally covered by a flange of the dentary. In lateral view, the suture between the angular and dentary is sinuous and that between the angular and supra-angular is nearly straight. Corresponding to the articulation for the quadrate, the angular has a large notch in the dorsal margin of its posterior portion. There is a dorsoventrally directed groove on the posterior part of the angular (Figs 4, 5), which represents the 'posterior mandibular pit-line' of Wenz (1967). A similar pit-line is also present in other ionoscopiforms (e.g. *O. muensteri*, Lane & Ebert, 2012, 2015; *Robustichthys*, Xu *et al*., 2014). This pit-line does not connect the preopercular sensory canal, different from the vertical branch of the mandibular canal in *Amia* (Grande & Bemis, 1998).

The retroarticular is small, and sutured to the posteroventral corner of the angular (Fig. 5).

Medially, two coronoid bones, a prearticular, a coronomeckelian and an articular are discernible in each lower jaw. Both coronoids are small and elongate bones, bearing relatively large, conical teeth at their oral margins (Fig. 5).

The prearticular is large and V-shaped, medially covered by dense small teeth (Fig. 6).

The coronomeckelian is small and nodular-like, laterally contacting the middle portion of the angular (Fig. 6).

A small portion of the articular is partly exposed beneath the notch of the angular, but its complete shape is still unknown.

Opercular series

The preopercle is narrow and crescent shaped. The anterior margin of the preopercle contacts the suborbitals and quadratojugal, and its dorsal end is nearly in contact with the dermopterotic. The preopercular sensory canal runs dorsoventrally through the preopercle, with some posterior diverticulae at the ventral portion of the preopercle, indicated by a series of pores near the posterior margin of this bone.

Immediately posterior to the preopercle lie the rest of the opercular bones, including the opercle, subopercle and interopercle. The opercle is large and trapezoidal, 1.5–1.7 times deeper than long. The subopercle is relatively small, bearing a triangular anterodorsal process that inserts between the preopercle and opercle. This process is about one-third to half the depth of the opercle. The interopercle is small and triangular, tapered anteroventrally.

Gular and branchiostegal rays

The median gular is elongate and nearly triangular, having a pointed anterior tip and a broad, convex posterior end. Its length is slightly over half the length of the lower jaw.

Fourteen pairs of branchiostegal rays are present (Figs 3, 4). They are elongate and plate-like, increasing in length and width posteriorly.

Liu *et al*. (2003) failed to identify the median gular, although this bone is present in their studied specimen (Fig. 2). Additionally, Liu *et al*. (2003) inaccurately estimated that *Asialepidotus* has ten pairs of branchiostegal rays.

Paired girdles and fins

A posttemporal, a presupracleithrum, a supracleithrum, a cleithrum, three postcleithra and two clavicle elements are present at each side of the pectoral girdle.

The posttemporal is sub-triangular, tapered medially, with a round posterolateral corner. Each posttemporal contacts the extrascapulars anteriorly and the supracleithrum laterally.

The presupracleithrum is small and sub-circular, lying between the posttemporal, the opercle and the supracleithrum. Although a presupracleithrum is absent in the living bowfin, this bone is present in many primitive halecomorphs, such as *Watsonulus* (Grande & Bemis, 1998), *C. furcatus* (Lambers, 1992; Grande & Bemis, 1998), *Robustichthys* (Xu *et al*., 2014) and *Panxianichthys* (Xu & Shen, 2015).

The supracleithrum is deep and anteriorly inclined, with its anterior portion slightly overlapped by the opercle.

The cleithrum is large and sickle shaped, bearing a series of curved ridges on the lateral surface of this bone. Small denticles are densely arranged on these ridges (Figs 4, 5). The anterior arm of the cleithrum is shorter than the dorsal arm (Fig. 5), showing a primitive condition, as in *Watsonulus* and other ionoscopiforms. In contrast, the anterior arm of the cleithrum is significantly longer than the dorsal arm in the Amiiformes (Grande & Bemis, 1998).

There are three plate-like postcleithra associated with the cleithrum. The dorsal is largest, as deep as the supracleithrum; the middle is trapezoidal, nearly one-third of the size of the dorsal; and the ventral is smallest and triangular.

There are two clavicle elements (Fig. 5). They are small and elongate, bearing several rows of denticles similar to those of the cleithrum. Two clavicle elements are otherwise known in *Ionoscopus* (Lambers, 1992), some amiiforms (*Amia*, *Amiopsis*, *Solnhofenamia* and *Amblysemius*; Grande & Bemis, 1998) and gars (Grande, 2010).

The pectoral fins are large, inserting low on the body. Each pectoral fin bears 15 distally segmented rays (Fig. 8B). The first is unbranched, preceded by one or two basal fulcra, and a series of fringing fulcra are associated with the leading ray. The remaining rays are branched distally. Given that the pectoral fins were incompletely preserved in the holotype, Su (1959) inaccurately estimated that *Asialepidotus* has only seven rays in each pectoral fin. Liu *et al*. (2003) made no descriptions of the pectoral fins.

The pelvic girdles are not exposed. The pelvic fins insert at the 12th or 13th vertical scale row. Each bears nine distally segmented rays, preceded by two or three basal fulcra and a series of fringing fulcra (Fig. 8C). The first ray is unbranched, and the others are branched distally. Su (1959) did not distinguish the basal fulcra from rays and miscounted that 11 rays were present in each pelvic fin.

Median fins

The dorsal fin originates above the 25th–26th vertical scale row. It is triangular and composed of ten or 11 principal rays (Fig. 8D). The first principal ray is distally segmented and unbranched, preceded by a rudimentary ray, three or four basal fulcra and a series of fringing fulcra; the remaining rays are branched distally. The rudimentary ray is about half of the length of the first principal ray.

The anal fin originates below the 22th–24th vertical scale row. It has 11–12 distally segmented principal rays (Fig. 8F). The first ray is unbranched, preceded by one rudimentary ray, two basal fulcra and a series of fringing fulcra, and the remaining rays are branched distally. The rudimentary ray is relatively short, two-fifths of the length of the first principal ray, and is composed of two segments, with the distal one inserting between two fringing fulcra.

The caudal fin is hemi-heterocercal, with a moderately forked profile (Fig. 8E). It has 21–23 principal rays. The dorsal marginal principal ray is segmented and unbranched in most specimens. In IVPP V20676, however, this ray is also branched, showing a condition similar to that in *O. muensteri* (Lane & Ebert, 2012, 2015). The ventral marginal principal ray is segmented and unbranched, and its length varies considerably in different specimens; the ratio of the length of the ventral marginal principal ray to that of the adjacent branched ray varies from one-half to one. The middle principal rays are segmented and branched up to four times. Additionally, nine or ten basal fulcra are present in the dorsal lobe, and two basal fulcra and three or four rudimentary rays in the ventral lobe. Fringing fulcra are present in both lobes.

Su (1959) correctly identified 11 anal fin rays in the holotype but did not describe the dorsal and caudal fins. Liu *et al*. (2003) correctly identified 11 dorsal fin rays and 22 principal caudal fin rays in his studied specimens, but he did not describe the anal fin.

Scales

The body is fully covered with rhombic scales. The scales are arranged in 43–45 vertical rows along the main lateral line. In addition, 10–13 rows of scales extend into the epaxial lobe of the caudal fin. The scales in the anterior flank region are 1.5 times deeper than wide, and they gradually become shorter and smaller dorsally, ventrally and posteriorly. In addition to the main lateral line, there is an additional lateral line, indicated by a line of seven or eight small pores on the scales in the predorsal region. A similar condition is also present in several other ionoscopiforms (e.g. *Ophiopsis procera*, Bartram, 1975; *Robustichthys*, Xu *et al*., 2014; *Subortichthys*, Ma & Xu, 2017). Most of the scales, except those covering the epaxial lobe of the caudal fin, have a serrated posterior margin, with 2–14 acute projections. The surfaces of the scales are largely smooth except for small pores and ridges on some scales. Pegs and anterodorsal extensions are exposed on some scales in the anterior flank region.

The trunk was broken into two parts in the holotype, with a few vertical rows of scales missing; Su (1959) estimated that *Asialepidotus* has ~40 vertical rows of scales along the lateral line.

PHYLOGENETIC ANALYSIS

To illuminate the phylogenetic position of *Asialepidotus* within the Holostei, a phylogenetic analysis was performed based on a data matrix expanded from Ma & Xu (2017), which in turn was derived from Grande & Bemis (1998), Xu *et al*. (2014) and Xu & Shen (2015). The present data matrix (see Part S2 in Supporting Information) includes 115 characters coded for 32 taxa. Characters 1–69 were adopted or slightly modified from Grande & Bemis (1998). The additional 46 characters were derived from other sources (e.g. Gardiner & Schaeffer, 1989; Gardiner *et al*., 1996; Coates, 1999; Arratia, 1999, 2013; Cavin & Suteethorn, 2006; Alvarado-Ortega & Espinosa-Arrubarrena, 2008; Cavin, 2010; Grande, 2010; Xu & Gao, 2011; Xu *et al*., 2012; López-Arbarello, 2012; Brito & Alvardo-Ortega, 2013, Cavin *et al*., 2013; Deesri *et al*., 2014; Xu, Gao & Coates, 2015; Xu & Shen, 2015; Xu & Zhao, 2016; Xu & Ma, 2016). All characters were unordered and equally weighted. The potential ionoscopiform *Archaeosemionotus* (López-Arbarello, Stockar & Bürgin, 2014) was not included because some phylogenetically important features are unclear in this taxon. The stem-neopterygian *Teffichthys* ('*Perleidus*') *madagascariensis* (Lehman, 1952; Marramà *et al*., 2017) was used as the outgroup taxon.

Phylogenetic analysis recovered six most parsimonious trees (tree length = 240 steps, consistency index (CI) = 0.5542, retention index = 0.7338). In the strict consensus tree (Fig. 9), Parasemionotiformes (represented by *Watsonulus eugnathoides*) are recovered in a basal position within the Halecomorphi, and Ionoscopiformes form the sister group of Amiiformes, as also found in other analyses (Grande & Bemis, 1998; Alvarado-Ortega & Espinosa-Arrubarrena, 2008; Xu *et al*., 2014; Xu & Shen, 2015; Ma & Xu, 2017). The results of our analysis suggest that the order 'Panxianichthyiformes' is paraphylectic; *Asialepidotus* is not a sister taxon of *Panxianichthys* as previously suggested by Sun *et al*. (2017); instead, it is more derived than *Panxianichthys* and consists of a sister taxon of the clade *Robustichthys* plus all Jurassic–Cretaceous ionoscopiforms.

Asialepidotus possesses two halecomorph synapomorphies, a symplectic articulating with the lower jaw, and a notched posterior margin of the maxilla. Within this clade, *Asialepidotus* is placed in the Ionoscopiformes because it possesses three derived features of the order: presence of a sensory canal in the maxilla, presence of a relatively long parietal (absent in *Subortichthys*), and presence of a canal-bearing innerorbital flange of the dermosphenotic (absent in *Subortichthys* and *Panxianichthys*). However, it lacks two derived features of *Robustichthys* shared with Jurassic–Cretaceous ionoscopiforms, which are the absence of a distinct quadratojugal and presence of a posteriorly inclined posterior border of the last infraorbital.

DISCUSSION

Our revision of *Asialepidotus* supports that the early diversification of Ionoscopiformes had occurred latest by the Middle Triassic in China. In the past decades, Ionoscopiformes were mainly known from the Early Cretaceous of the New World (Shaeffer, 1960, 1971; Maisey, 1991; Brito, 2000; Alvarado-Ortega & Espinosa-Arrubarrena, 2008; Machado *et al*., 2013), the Late Jurassic of Europe (Bartram, 1975; Lane & Ebert, 2012, 2015) and the Middle Jurassic of Africa (Saint-Seine, 1955; Taverne, 2015). Although potential ionoscopiforms have also been reported from the late Middle Triassic of Italy and Austria (Sieber, 1955; López-Arbarello *et al*., 2014), they are based on poorly preserved specimens and need further studies. Recently, three ionoscopiforms based on well-preserved specimens (*Robustichthys*, *Panxianichthys* and *Subortichthys*) were successively reported from the early Middle Triassic (Pelsonian, Anisian, ~244 Mya; Hu *et al*., 2015) of Luoping, Yunnan, and Panxian, Guizhou (Xu *et al*., 2014; Xu & Shen, 2015; Ma & Xu, 2017). They document the oldest records of this order. The taxonomic reassessment of *Asialepidotus* herein extends the distribution of Chinese ionoscopiforms from Luoping and Panxian into Fuyuan and Xingyi, and further enriches our knowledge on the taxonomic diversity and geographical distribution of this group. As the age (late Ladinian, ~240 Mya; Li *et al*., 2016) of the fossil beds is well constrained, *Asialepidotus* documents the youngest ionoscopiform in China, extending the stratigraphic range of this group in China by ~4 Myr.

The Chinese ionoscopiforms are significantly older and more plesiomorphic than their relatives from Europe and other places, providing insights that this order probably originated in South China. In the Middle Triassic, almost all of the Earth's landmasses were combined in the supercontinent of Pangaea, surrounded by a vast ocean of Panthalassa, and an arm of this ocean called the Tethys (including the Palaeo-Tethys in the north and the Meso-Tethys in the south) intruded deeply into the centre of Pangaea at the equator (Metcalfe, 2011). South China was located at the eastern end of the Palaeo-Tethys Ocean, and Europe at the western end of this ocean. The Palaeo-Tethys Ocean would have provided an east–west corridor for dispersal and biological exchanges of ionoscopiforms between South China and Europe (Xu *et al*., 2014), as indicated by studies of other types of ray-finned fishes, marine reptiles and invertebrates (Li & Jin, 2009; Xu *et al*., 2012; Benton *et al*., 2013; Tintori *et al*., 2014).

Asialepidotus, represented by thousands of specimens (personal estimation), is the numerically dominant taxon in the late Middle Triassic Xingyi vertebrate fauna. Along with *Asialepidotus*, other halecomorphs in the same fauna include *Sinoeugnathus kueichowensis* (Su, 1959) and *Xingyia gracilis* (Liu *et al*., 2003); both taxa, although placed in the amiiform Caturidae, need further studies. No ginglymodians have so far been reported from this fauna; possible ginglymodians were mentioned by Jin (2009) based on a few specimens, but they have not yet been described. Considering the taphonomic nature and the multiple-year field collections at the localities, it is unlikely that this reflects a sampling bias; instead, it may well indicate that halecomorphs were richer than ginglymodians in number and probably had a more important palaeoecological role in this ecosystem.

Although *Asialepidotus* was included in a previous cladistic analysis (Sun *et al*., 2017), many of its characters previously were not available or not properly coded. Our redescription of *Asialepidotus* on the basis of a large number of well-preserved specimens provides more complete and precise information on its morphology than before. Of the 112 characters of Sun *et al*. (2017), 13 unknowns (characters 13, 24, 25, 58, 69, 77, 81, 82, 83, 84, 88, 90 and 110) can now be resolved unequivocally, and seven (characters 17, 21, 33, 61, 93, 102 and 104) can be coded differently. In contrast to the placement by Sun *et al*. (2017) of *Asialepidotus* in the 'Panxianichthyiformes' (below the Ionoscopiformes/Amiiformes split), the results of our analysis based on the new dataset strongly support the alternative placement of *Panxianichthys* and *Asialepidotus* successively at the base of the Ionoscopiformes. This revised topology is valuable for better understanding of the sequence of character acquisition in early ionoscopiform evolution.

Our studies show that 'Panxianichthyiformes' of Sun *et al*. (2017) is a poorly defined, paraphylectic grade. In the consensus tree of Sun *et al*. (2017), the 'panxianichthyiform' monophyly was weakly supported by three characters: (1) dermopterotic subrectangular, not substantially tapered anteriorly or widened posteriorly [character 33(1), consistency index (CI) = 0.200]; (2) body lobe scale row present, without additional incomplete row [character 109(2), CI = 0.500]; and (3) supramaxilla usually higher in the anterior region than in the posterior [character 111(1), CI = 0.333]. Our re-examinations show that both *Asialepidotus* and *Panxianichthys* have an anteriorly tapering dermopterotic, as in other ionoscopiforms; Sun *et al*. (2017) made inaccurate codings on the first character for both taxa. As for the second character, *Asialepidotus* and *Panxianichthys* have an incomplete last scale row, as in *Eoeugnathus* (Herzog, 2003), *Robustichthys* (Xu *et al*., 2014) and many other holosteans. Sun *et al*. (2017) made an inaccurate coding of this character for *Eoeugnathus* (see fig. 13 of Herzog, 2003). Among four genera united in the 'Panxianichthyiformes' by Sun *et al*. (2017), only *Allolepidotus* (Lombardo, 2001) probably has a complete last scale row, as in some ginglymodians (López-Arbarello, 2012). Thus, the second character cannot be a 'panxianichthyiform' synapomorphy. In addition, the third character is unlikely to be a 'panxianichthyiform' synapomorphy because it is widely distributed in early halecomorphs or even in some ginglymodians. The other diagnostic characters of 'Panxianichthyiformes' listed by Sun *et al*. (2017) are not based on the results of their phylogenetic analysis; most of them are primitive halecomorph features [e.g. presence of a symplectic articulation ventral to that of the quadrate (see discussion by Gardiner *et al*., 1996); up to three suborbitals; crescent-shaped preopercle; and ganoid scales all over the body], and two cannot be confirmed by our revision of *Asialepidotus* (see Palatine, hyoid and branchial series and Circumorbital bones in Description, above), i.e. presence of a plate-like quadratojugal between the preopercle and the quadrate, not sutured to the quadrate itself (*Panxianichthys* has a splint-like quadratojugal medially contacting the quadrate; G-H Xu, personal observation); and a dermosphenotic hinged to the side of the skull roof and with a smooth innerorbital flange, which bears no sensory canal.

CONCLUSION

Comparative studies of the original fossil material with 50 new specimens of *A. shingyiensis* have revealed a lot of new and detailed anatomical information for the skull (e.g. rostral, vomers, parasphenoid, small fenestra for palatine ramus of facial nerve in premaxilla, dermosphenotics, sphenotics, supraorbitals, suborbitals, sclerotic bones, palatine bones, quadratojugals, hyomandibulas, hypohyals, anterior and posterior ceratohyals, median gular, sensory canal in maxilla, and coronoids, prearticulars, retroarticulars and coronomeckelians in lower jaws), pectoral girdles, fins and scales. These new data have permitted a complete revision of the anatomy and life reconstruction of this taxon.

The results of our phylogenetic analysis incorporating new anatomical data for *Asialepidotus* recover this taxon as a basal ionoscopiform and provide new insights into the phylogenetic relationships of early halecomorphs. The monophyly of the poorly defined 'Panxianichthyiformes' is rejected. Moreover, the phylogenetic reassessment of *Asialepidotus* enriches our knowledge on the taxonomic diversity and geographical distribution of the Ionoscopiformes and extends the stratigraphic range of this group in China by ~4 Myr.

ACKNOWLEDGMENTS

We thank Yin Peng-Fei for conducting X-ray computed tomography, Lionel Cavin and two anonymous referees for helpful comments on an early version of the manuscript. The research was supported by the National Natural Science Foundation of China (NSFC grants 41672001, 41272002 and 41688103), and the Strategic Priority Research Program (B) of Chinese Academy of Sciences (grants XDB18000000 and 05010000), and the Key Research Program of Frontier Sciences of Chinese Academy of Sciences (grant QYZDB-SSW-DQC040).

REFERENCES

Alvarado-Ortega J, Espinosa-Arrubarrena L. 2008. A new genus of ionoscopiform fish (Halecomorphi) from the Lower Cretaceous (Albian) lithographic limestones of the Tlayúa quarry, Puebla, México. *Journal of Paleontology* **82:** 163–175.

Applegate SP. 1988. A new genus and species of a holostean belonging to the family Ophiopsidae, *Teoichthys kallistos*, from the Cretaceous near Tepexi de Rodríguez, Puebla. *Instituto de Geología, Revista* **7:** 200–205.

Argyriou T. 2017. Skeletal anatomy and systematic placement of the Permian actinopterygian *Brachydegma caelatum* based on new data from uCT. In: Murray AM, Holmes RB, eds. *Canadian Society of Vertebrate Palaeontology 2017 Abstracts*, 1–6. Doi: 10.18435/B5S3D.

Arratia G. 1999. The monophyly of Teleostei and stem-group teleosts. Consensus and disagreements. In: Arratia G, Schultze H-P, eds. *Mesozoic Fishes 2– Systematics and Fossil Record*. München: Verlag Dr. Pfeil, 265–334.

Arratia G. 2013. Morphology, taxonomy, and phylogeny of Triassic pholidophorid fishes (Actinopterygii, Teleostei). *Society of Vertebrate Paleontology Memoir (Supplement to Journal of Vertebrate Paleontology)* **13:** 1–138.

Bartram AWH. 1975. The holostean fish genus *Ophiopsis* Agassiz. *Zoological Journal of the Linnean Society* **56:** 183–205.

Benton MJ, Zhang Q-Y, Hu S-X, Chen Z-Q, Wen W, Liu J, Huang J-Y, Zhou C-Y, Xie T, Tong J-N, Choo B. 2013. Exceptional vertebrate biotas from the Triassic of China, and the expansion of marine ecosystems after the Permo-Triassic mass extinction. *Earth-Science Reviews* **125:** 199–243.

Brito PM. 2000. A new halecomorph with two dorsal fins, *Placidichthys bidorsalis* n. g., n. sp. (Actinopterygii: Halecomorphi) from the Lower Cretaceous of the Araripe Basin, northeast Brazil. *Earth and Planetary Sciences* **331:** 749–754.

Brito PM, Alvarado-Ortega J. 2013. *Cipactlichthys scutatus*, gen. nov., sp. nov. a new Halecomorph (Neopterygii, Holostei) from the Lower Cretaceous Tlayua Formation of Mexico. *PLoS ONE* **8:** e73551.

Broughton RE, Betancur-R R, Li C, Arratia G, Ortí G. 2013. Multi-locus phylogenetic analysis reveals the pattern and tempo of bony fish evolution. *PLOS Currents Tree of Life*. Apr 16. Edition 1. Doi: 10.1371/currents.tol.2ca8041495ffafd0c92756e75247483e.

Cavin L. 2010. Diversity of Mesozoic semionotiform fishes and the origin of gars (Lepisosteidae). *Die Naturwissenschaften* **97:** 1035–1040.

Cavin L, Deesri U, Suteethorn V. 2013. Osteology and relationships of *Thaiichthys* nov. gen.: a Ginglymodi from the Late Jurassic–Early Cretaceous of Thailand. *Palaeontology* **56:** 183–208.

Cavin L, Suteethorn V. 2006. A new Semionotiform (Actinopterygii, Neopterygii) from Upper Jurassic–Lower Cretaceous deposits of North-East Thailand, with comments on the relationships of Semionotiforms. *Palaeontology* **49:** 339–353.

Chang M-M, Jin F. 1996. Mesozoic fish faunas from China. In: Arratia G, Viohl G, eds. *Mesozoic Fishes: Systematics and Paleoecology*. Munich: Verlag Dr. F. Pfeil, 461–478.

Chang M-M, Miao D-S. 2004. An overview of Mesozoic fishes in Asia. In: Arratia G, Tintori A, eds. *Mesozoic Fishes 3: Systematics, Paleoenvironments and Biodiversity.* Munich: Verlag Dr. Friedrich Pfeil, 535–563.

Chen Z. 1985. Stratigraphical position of *Keichousaurus hui* from the Middle Triassic of southwestern Guizhou and its significance. *Guizhou Geology* **5:** 289–290.

Coates MI. 1999. Endocranial preservation of a Carboniferous actinopterygian from Lancashire, UK, and the interrelationships of primitive actinopterygians. *Philosophical Transactions of the Royal Society B: Biolocial Sciences* **354:** 435–462.

Deesri U, Lauprasert K, Suteethorn V, Wongko K, Cavin L. 2014. A new species of the ginglymodian fish *Isanichthys* from the Late Jurassic Phu Kradung Formation, northeastern Thailand. *Acta Palaeontologica Polonica* **59:** 313–331.

Friedman M. 2015. The early evolution of ray-finned fishes. *Palaeontology* **58:** 213–228.

Gardiner BG. 1960. A revision of certain actinopterygian and coelacanth fishes, chiefly from the Lower Lias. *Bulletin of the British Museum (Natural History), Geology* **4:** 239–384.

Gardiner BG. 1984. The relationships of the palaeoniscid fishes, a review based on new specimens of *Mimia* and *Moythomasia* from the Upper Devonian of western Australia. *Bulletin of the British Museum (Natural History), Geology* **37:** 173–428.

Gardiner BG, Maisey JG, Littlewood DTJ. 1996. Interrelationships of basal neopterygians. In: Stiassney MLJ, Parenti LR, Johnson GD, eds. *Interrelationships of fishes*. San Diego: Academic Press, 117–146.

Gardiner BG, Schaeffer B. 1989. Interrelationships of lower actinopterygian fishes. *Zoological Journal of the Linnean Society* **97:** 135–187.

Geng B-H, Zhu M, Jin F. 2009. A revision and phylogenetic analysis of *Guizhoucoelacanthus* (Sarcopterygii, Actinistia) from the Triassic of China. *Vertebrata PalAsiatica* **47:** 165–177.

Gill EL. 1923. The Permian fishes of the genus *Acentrophorus*. *Proceedings of the Zoological Society of London* **93:** 19–40.

Goodrich ES. 1930. *Studies on the structure and development of vertebrates*. London: Macmillan.

Grande L. 2010. An empirical synthetic pattern study of gars (Lepisosteiformes) and closely related species, based mostly on skeletal anatomy. The resurrection of Holostei. *Copeia* **10 (Supplement):** 1–871.

Grande L, Bemis WE. 1998. A comprehensive phylogenetic study of amiid fishes (Amiidae) based on comparative skeletal anatomy: An empirical search for interconnected patterns of natural history. *Society of Vertebrate Paleontology Memoir (supplement to Journal of Vertebrate Paleontology)* **4:** 1–690.

Herzog A. 2003. Eine Neubeschreibung der Gattung *Eoeugnathus* Brough, 1939 (Actinopterygii; Halecomorphi) aus der alpinen Mitteltrias Grau bündens (Schweiz). *Paläontologische Zeitschrift* **77:** 201–218.

Hu S-X, Zhang Q-Y, Wen W, Huang J-Y, Zhou C-Y, Xie T, Lü T, Liu T-L, Benton MJ. 2015. *The Luoping biota: A taphonomic window on Triassic biotic recovery and radiation*. Kunming: Yunnan Science & Technology Press.

Hurley IA, Mueller RL, Dunn KA, Schmidt EJ, Friedman M, Ho RK, Prince VE, Yang ZH, Thomas MG, Coates MI. 2007. A new time-scale for ray-finned fish evolution. *Proceedings of the Royal Society B: Biological Sciences* **274:** 489–498.

Huxley TH. 1861. Preliminary essay upon the systematic arrangement of the fishes of the Devonian epoch. *Memoirs of the Geological Survey of the United Kingdom, Decade* **10:** 1–40.

Inoue JG, Miya M, Tsukamoto K, Nishida M. 2003. Basal actinopterygian relationships: a mitogenomic perspective on the phylogeny of the "ancient fish". *Molecular Phylogenetics and Evolution* **26:** 110–120.

Jin F. 2001. Notes on the discovery of *Birgeria* in China. *Vertebrata Palasiatica* **39:** 168–176.

Jin F. 2006. An overview of Triassic fishes from China. *Vertebrata PalAsiatica* **44:** 28–42.

Jin F. 2009. Fishes. In: Li J-L, Jin F, eds. *Swimming in the ocean two hundred million years ago: Triassic marine reptile and environment of South China*. Beijing: Science Press, 99–121.

Lambers PH. 1992. On the Ichthyofauna of the Solnhofen lithographic limestone (Upper Jurassic, Germany). Unpublished D. Phil. Thesis, Rijksuniversiteit Groningen.

Lane JA, Ebert M. 2012. Revision of *Furo muensteri* (Halecomorphi, Ophiopsidae) from the Upper Jurassic of western Europe, with comments on the genus. *Journal of Vertebrate Paleontology* **32:** 799–819.

Lane JA, Ebert M. 2015. A taxonomic reassessment of *Ophiopsis* (Halecomorphi, Ionoscopiformes), with a revision of Upper Jurassic species from the Solnhofen Archipelago, and a new genus of Ophiopsidae. *Journal of Vertebrate Paleontology* **35:** e883238.

Lehman JP. 1952. Étude complémentaire des poissons de l'Eotrias de Madagascar. *Kungliga Svenska Vetenskapsakademiens Handlingar* **2:** 1–201.

Li C, Wu X-C, Zhao L-J, Nesbitt SJ, Stocker MR, Wang L-T. 2016. A new armored archosauriform (Diapsida: Archosauromorpha) from the marine Middle Triassic of China, with implications for the diverse life styles of archosauriforms prior to the diversification of Archosauria. *The Science of Nature* **103:** 95.

Li J-L. 2006. A brief summary of the Triassic marine reptiles of China. *Vertebrata PalAsiatica* **44:** 99–108.

Li J-L, Jin F. 2003. New advances of the research on *Keichousaurus* reptile fauna. *Progress in Natural Sciences* **13:** 796–800.

Li J-L, Jin F. 2009. *Swimming in the ocean two hundred million years ago: Triassic marine reptile and environment of South China*. Beijing: Science Press.

Li Z-G, Sun Z-Y, Jiang D-Y, Ji C. 2016. LA-ICP-MS Zircon U-Pb age of the fossil layer of Triassic Xingyi Fauna from Xingyi, Guizhou, and its Significance. *Geological Review* **62:** 779–790.

Liem KF, Bemis WE, Walker WF, Grande L. 2001. *Functional anatomy of the vertebrates: an evolutionary perspective,* 3rd edn. Fort Worth, Texas: Harcourt College Publishers.

Liu G-B. 2004. Changing names: *Guizhoueugnathus*, new name for *Guizhouella* Liu, 2003 and *Guizhoubrachysomus*, new name for *Brachysomus* Liu, 2003. *Acta Palaeontologica Sinica* **43:** 447.

Liu G-B, Yin G-Z, Wang X-H. 2002. On the most primitive amiid fish from Upper Triassic of Xingyi, Guizhou. *Acta Palaeontological Sinica* **41:** 461–463.

Liu G-B, Yin G-Z, Wang X-H, Luo Y-M, Wang S-Y. 2003. New discovered fishes from *Keichousaurus* bearing horizon of Late Triassic in Xingyi of Guizhou. *Acta Palaeontologica Sinica* **42:** 346–366.

Lombardo C. 2001. Actinopterygians from the Middle Triassic of northern Italy and Canton Ticino (Switzerland): anatomical descriptions and nomenclatural problems. *Rivista Italiana di Paleontologia e Stratigrafia* **107:** 345–369.

López-Arbarello A. 2012. Phylogenetic interrelationships of ginglymodian fishes (Actinopterygii: Neopterygii). *PLoS ONE* **7:** e39370.

López-Arbarello A, Stockar R, Bürgin T. 2014. Phylogenetic relationships of the Triassic *Archaeosemionotus* Deecke (Halecomorphi, Ionoscopiformes) from the 'Perledo fauna'. *PLoS ONE* **9:** e108665.

Ma X-Y, Xu G-H. 2017. A new ionoscopiform fish (Holostei: Halecomorphi) from the Middle Triassic (Anisian) of Yunnan, China. *Vertebrata PalAsiatica* **55:** 92–106.

Machado GP, Alvarado-Ortega J, Machado LP, Brito PM. 2013. *Teoichthys brevipina*, sp. nov., a new ophiopsid fish (Halecomorphi, Ionoscopiformes) from the Lower Cretaceous Tlayúa Formation, Central Mexico. *Journal of Vertebrate Paleontology* **33:** 482–487.

Maisey JG. 1991. *Oshunia* Wenz and Kellner, 1986. In: Maisey JG, ed. *Santana fossils: an illustrated atlas*. New York: TFH Publications Inc., 157–168.

Marramà G, Lombardo C, Tintori A, Carnevale G. 2017. Redescription of '*Perleidus*' (Osteichthyes, Actinopterygii) from the Early Triassic of northwestern Madagascar. *Rivista Italiana di Paleontologia e Stratigrafia* **123:** 219–242.

Metcalfe I. 2011. Palaeozoic–Mesozoic history of SE Asia. In: Hall R, Cottam MA, Wilson MEJ, eds. *The SE Asian gateway: history and tectonics of the Australia–Asia collision*. London: Geological Society, Special Publications, No. 355, 7–35.

Nakatani M, Miya M, Mabuchi K, Saitoh K, Nishida M. 2011. Evolutionary history of Otophysi (Teleostei), a major clade of the modern freshwater fishes: Pangaean origin and Mesozoic radiation. *BMC Evolutionary Biology* **11:** 177.

Near TJ, Eytan RI, Dornburg A, Kuhn KL, Moore JA, Davis MP, Wainwright PC, Friedman M, Smith WL. 2012. Resolution of ray-finned fish phylogeny and timing of diversification. *Proceedings of the National Academy of Sciences of the United States of America* **109:** 13698–13703.

Nelson GJ. 1969. Infraorbital bones and their bearing on the phylogeny and geography of osteoglossomorph fishes. *American Museum Novitates* **2394:** 1–37.

Nelson JS. 2006. *Fishes of the World*, *4th edn*. Hoboken, NJ: John Wiley and Sons, Inc.

Nelson JS, Grande TC, Wilson MVH. 2016. *Fishes of the World*, *5th edn*. Hoboken, NJ: John Wiley and Sons, Inc.

Olsen PE. 1984. The skull and pectoral girdle of the parasemionotid fish *Watsonulus eugnathoides* from the Early Triassic Sakamena Group of Madagascar, with comments on the relationship of the holostean fishes. *Journal of Vertebrate Paleontology* **4:** 481–499.

Olsen PE, McCune AR. 1991. Morphology of the *Semionotus elegans* species group from the Early Jurassic part of the Newark supergroup of eastern North America with comments on the family Semionotidae (Neopterygii). *Journal of Vertebrate Paleontology* **11:** 269–292.

Patterson C. 1973. Interrelationships of holosteans. In: Greenwood PH, Miles RS, Patterson C, eds. *Interrelationships of fishes*. London: Academic Press, 233–305.

Rayner DH. 1948. Structure of certain Jurassic holostean fishes with special reference to their neurocrania. *Philosophical Transactions of the Royal Society of London, Series B, Biological Sciences* **233:** 287–345.

Regan CT. 1923. The skeleton of *Lepidosteus*, with remarks on the origin and evolution of the lower neopterygian fishes. *Proceedings of the Zoological Society of London* **93:** 445–461.

Romer AS. 1945. *Vertebrate Paleontology, 2nd edn*. Chicago: University of Chicago Press.

Rosen DE, Forey PL, Gardiner BG, Patterson C. 1981. Lungfishes, tetrapods, paleontology and plesiomorphy. *Bulletin of the American Museum of Natural History* **167:** 159–4276.

Saint-Seine P. 1949. Les poissons des calcaires lithographique de Cerin (Ain). *Nouvelles archives du Muséum (national) d'histoire naturelle, Lyon* **2:** 1–357.

Saint-Seine P. 1955. Poissons fossiles de l'étage de Stanleyville (Congo Belge). Premiere partie: la faune des argilites et schistes bitumineux. *Annales du Musée Royal du Congo Belge, Tervuren (Belgique), Série in-8°, Sciences Géologiques* **14:** 1–126.

Schaeffer B. 1960. The Cretaceous holostean fish *Macrepistius*. *American Museum Novitates* **2011:** 1–18.

Schaeffer B. 1971. The braincase of the holostean fish *Macrepistius*, with comments on neurocranial ossification in the Actinopterygii. *American Museum Novitates* **2459:** 1–34.

Schultze H-P. 1993. Patterns of diversity in the skulls of jawed fishes. In: Hanken J, Hall BK, eds. *The skull, Vol. 2, Patterns of structural and systematic diversity.* Chicago: University of Chicago Press, 189–254.

Sieber R. 1955. Ein bemerkenswerter Fischfund aus der Mitteltrias Kärtens. *Carinthia* **2:** 91–96.

Su D-Z. 1959. Triassic fishes from Kueichow, Southwest China. *Vertebrata PalAsiatica* **3:** 205–210.

Sun Z-Y, Tintori A, Xu Y-Z, Cristina L, Ni P-G, Jiang D-Y. 2017. A new non-parasemionotiform order of the Halecomorphi (Neopterygii, Actinopterygii) from the Middle Triassic of Tethys. *Journal of Systematic Palaeontology* **15:** 223–240.

Swofford DL. 2003. *PAUP*. Phylogenetic analysis using parsimony (*and other methods). Version 4.0b10*. Sunderland, MA: Sinauer Associates.

Taverne L. 2015. Osteology and phylogenetic relationships of *Congophiopsis lepersonnei* gen. nov. (Halecomorphi, Ionoscopiformes) from the Songa Limestones (Middle Jurassic, Stanleyville Formation), Democratic Republic of Congo. *Geo-Eco-Trop* **38:** 223–240.

Tintori A, Hitij T, Jiang D, Lombardo C, Sun Z. 2014. Triassic actinopterygian fishes: the recovery after the end-Permian crisis. *Integrative Zoology* **9:** 394–411.

Tintori A, Sun Z-Y, Ni P-G, Lombardo C, Jiang D-Y, Ryosuke M. 2015. Oldest stem Teleostei from the late Ladinian (Middle Triassic) of southern China. *Rivista Italiana di Paleontologia e Stratigrafia* **121:** 285–296.

Wang C-Y, Kang P-Q, Wang Z-H. 1998. Conodont-based age of the *Keichousaurus hui Yang*, 1958. *Acta Micropalaeontologica Sinica* **15:** 196–198.

Wenz S. 1967. *Compléments é l'étude des poissons Actinoptérygiens du Jurassique français*. Paris: Cahiers de Paléontologie, CNRS.

Westoll TS. 1944. The Haplolepidae, a new family of Late Carboniferous bony fishes – a study in taxonomy and evolution. *Bulletin of the American Museum of Natural History* **83:** 1–121.

Xu G-H, Gao K-Q. 2011. A new scanilepiform from the Lower Triassic of northern Gansu Province, China, and phylogenetic relationships of non-teleostean Actinopterygii. *Zoological Journal of the Linnean Society* **161:** 595–612.

Xu G-H, Gao K-Q, Coates MI. 2015. Taxonomic revision of *Plesiofuro mingshuica* from the Lower Triassic of northern Gansu, China, and the relationships of early neopterygian clades. *Journal of Vertebrate Paleontology* **35:** e1001515.

Xu G-H, Ma X-Y. 2016. A Middle Triassic stem-neopterygian fish from China sheds new light on the peltopleuriform phylogeny and internal fertilization. *Science Bulletin* **61:** 1766–1774.

Xu G-H, Ma X-Y. 2017. Taxonomic revision of *Asialepidotus shingyiensis* Su, 1959 (Halecomorphi, Holostei) from the Middle Triassic (Ladinian) of Guizhou and Yunnan, China. *Research & Knowledge* **3:** 36–38.

Xu G-H, Shen C-C. 2015. *Panxianichthys imparilis* gen. et sp. nov., a new ionoscopiform (Halecomorphi) from the Middle Triassic of Guizhou, China. *Vertebrata PalAsiatica* **53:** 1–15.

Xu G-H, Wu F-X. 2012. A deep-bodied ginglymodian fish from the Middle Triassic of eastern Yunnan Province, China, and the phylogeny of lower neopterygians. *Chinese Science Bulletin* **57:** 111–118.

Xu G-H, Zhao L-J. 2016. A Middle Triassic stem-neopterygian fish from China shows remarkable secondary sexual characteristics. *Science Bulletin* **61:** 338–344.

Xu G-H, Zhao L-J, Coates MI. 2014. The oldest ionoscopiform from China sheds new light on the early evolution of halecomorph fishes. *Biology Letters* **10:** 20140204.

Xu G-H, Zhao L-J, Gao K-Q, Wu F-X. 2012. A new stem-neopterygian fish from the Middle Triassic of China shows the earliest over-water gliding strategy of the vertebrates. *Proceedings of the Royal Society B: Biological Sciences* **280:** 20122261.

Xu G-H, Zhao L-J, Shen C-C. 2015. A Middle Triassic thoracopterid from China highlights the evolutionary origin of over-water gliding in early ray-finned fishes. *Biology Letters* **11:** 20140960.

Young C-C. 1958. On the new pachypleurosauroidea from Keichow, South-West China. *Vertebrata PalAsiatica* **2:** 69–81.

Zou X-D, Balini M, Jiang D-Y, Tintori A, Sun Z-Y, Sun Y-L. 2015. Ammonoids from the Zhuganpo Member of the Falang Formation at Nimaigu and their relevance for dating the Xingyi Fossil-Lagerstaette (Late Ladinian, Guizhou, China). *Rivista Italiana di Paleontologia e Stratigrafia* **121:** 135–161.

SUPPORTING INFORMATION

Additional Supporting Information may be found in the online version of this article at the publisher's web-site:

Supporting Information S1. Character list.
Supporting Information S2. Character–taxon matrix used for phylogenetic analysis.
Supporting Information S3. The strict consensus tree with character states supporting the nodes and terminal taxa.
Supporting Information S4. References.